Research article

Variation and health risks of the potentially toxic metals in dust around an industrial hub

Heleen C. Vos[1,2*], Kaukurauee I. Kangueehi[1], René Toesie[3], Grant Ravenscroft[4], Susanne Fietz[1]

[1]Department of Earth Sciences, University of Stellenbosch, Stellenbosch, 7600, South Africa
[2]BIOGRIP Water and Soil Node, University of Stellenbosch, Stellenbosch, 7600, South Africa
[3]Saldanha Bay Municipality, Vredenburg, 7380, South Africa
[4]Argos Scientific Pty Ltd., Cape Town, 7405, South Africa
*Corresponding author: heleenvos@sun.ac.za

Received: 14 May 2025 - **Reviewed:** 18 July 2025 - **Accepted:** 17 November 2025
https://doi.org/10.17159/caj/2025/35/2.22227

Abstract

The port area around Saldanha Bay, South Africa, is an industrial hub that processes large quantities of mining material and produces metals and steel, which leads to the visible emission of industrial dust. This study addresses the spatial and temporal variation of potentially toxic metals in the dust surrounding the industrial hub of Saldanha Bay and the potential health risks associated with them. Monitoring by the Saldanha Bay Municipality using dust buckets gives insight into the monthly Fe, Mn, Cu, Pb, and Zn content and deposition fluxes from 2016 to 2023. In addition, an extended sampling effort with Big Spring Number Eight (BSNE) samplers allowed us to additionally determine the Al, As, Ba, Cd, Co, Cr, Mo, Ni, Sb, Se, Sn, Sr, and V content in the dust particles. Results showed that in general, the Fe, Mn and Zn fluxes increased over time while the Pb flux decreased. Health risk indices suggest that the Pb and Mn content in the dust particles could pose a significant risk to public health. Certain regions in the study area are at higher risk than others, illustrating the need to monitor the spatial variability. Furthermore, the content of Co, Cu, Mn, and Ni is high compared to published concentrations in other urban areas around the world. Future work could investigate the precise origin of each metal to develop appropriate mitigation plans and protect public health in such industrial areas.

Keywords

Air pollution; dust deposition; toxic metals; health risk assessment; industry

Introduction

Air pollution is considered an important environmental threat to human health worldwide, causing around 6.7 million premature deaths annually (Health Effects Institute, 2020; WHO, 2021). One important cause of air pollution is the emission of dust particles by anthropogenic activities such as industry, mining, energy production, and traffic. The health risks of the dust particles emitted by such activities are determined by the quantity of particles, as well as the presence of potentially toxic metals like Pb, Zn, Cr, and Mn, among others (Nan et al., 2023; WHO, 2021, 2016; Yan et al., 2025). The global emission of dust and toxic metals associated with industries and mining has greatly increased in the last century due to land-use changes and an increase in production and industrialisation (Han et al., 2002; Hooper and Marx, 2018; McConnell and Edwards, 2008; Nriagu, 1996; Tian et al., 2015; Wan et al., 2016). To mitigate the harmful effects of toxic metals in dust, the possible sources of these metals and the risk they pose to public health must be understood (Li et al., 2019).

Saldanha Bay is located on the west coast of South Africa and hosts an important export hub and industrial development zone. Several industrial activities take place in the area, including ore transport, smelting, and steel galvanising. Annually, around 55.2 million tons of Fe ore and 4.7 million tons of Mn ore are exported, in addition to the processing of lead, zinc, copper, and galvanised steel (AEC, 2022). Concerns have been raised about possible air pollution caused by these industries and the impacts on public health. The Fe ore transport, processing, and storage have drawn particular attention due to the generation of visible red dust dispersed throughout the area. However, other operations such as ore processing and steel production

could also emit particles containing potentially toxic metals, as has been reported from operations around the world (Al-Swadi et al., 2022; Entwistle et al., 2019; Nelson, 2013; Utembe et al., 2015; Zheng et al., 2010). Further industrial development is planned in the Saldanha Bay area (AEC, 2022), increasing the possible negative health risk.

Monitoring by the Saldanha Bay Municipality targets both the concentration of particles smaller than 2.5 µm ($PM_{2.5}$) and the total deposition of dust. The $PM_{2.5}$ concentrations and dust deposition data have been analysed by Vos et al. (2024) and suggest a low risk for public health in the Saldanha Bay Municipality. However, the potentially toxic metal content of the dust, which has generally been associated with a negative impact of industrial dust on public health, had not yet been considered. Understanding the metal content of the dust, and not just the quantity of dust, will contribute to improved knowledge of the health risks associated with such an industrial hub.

This study investigates the metal content of the dust in Saldanha Bay, with a focus on its temporal and spatial variability and potential public health impacts. The Saldanha Bay Municipality has been conducting dust monitoring in line with the national air monitoring guidelines (DEA, 2017), measuring the long-term total dust deposition flux and analysing the Fe, Mn, Zn, Cu, and Pb content in the dust. We extended this monitoring effort by collecting additional total dust samples and analysing an expanded suite of metals. We focus on metals commonly associated with industrial activities and mining, and known to threaten public health (Al-Swadi et al., 2022; Briffa et al., 2020; Chen et al., 2022; Okanigbe et al., 2017; Ondrasek et al., 2025; Zheng et al., 2020). Altogether, this study targets Al, As, Ba, Cd, Co, Cr, Cu, Fe, Mn, Mo, Ni, Pb, Sb, Se, Sn, Sr, V, and Zn. The study aims to (a) quantify the concentration of metals and the metal flux in the dust in residential areas surrounding the port, (b) determine the temporal and spatial variability of the metal fluxes, and (c) evaluate the health risks associated with potentially toxic metals in the dust. We also propose recommendations for improving this assessment and identify further research to more accurately evaluate the health impact of air pollution.

Material and methods

Study area

The Saldanha Bay Municipality is located on the west coast of

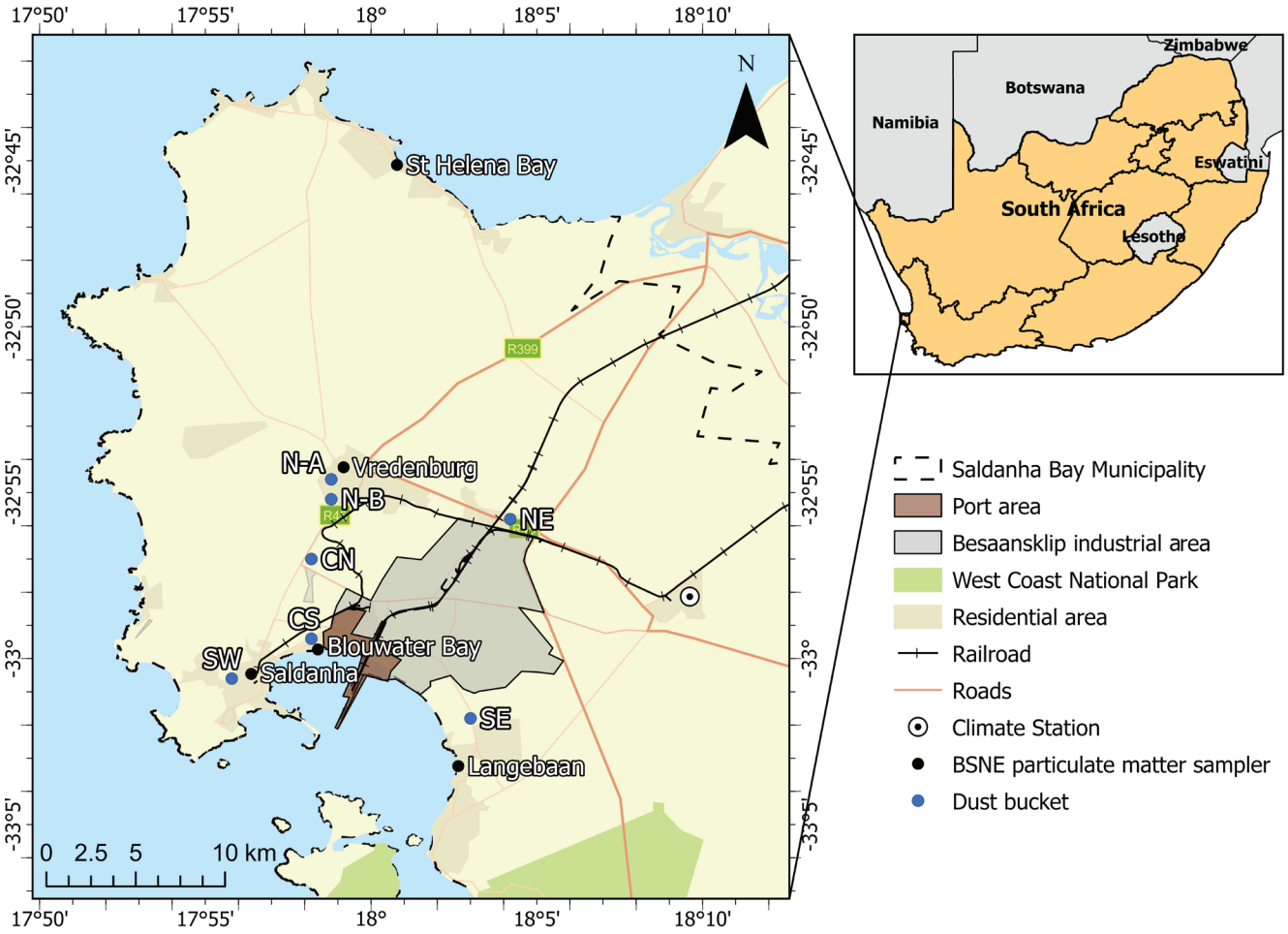

Figure 1: *Map of the study area indicating the location of the dust buckets, the BSNE samplers, the climate station, and major industrial areas. Ground map provided by ESRI (World Street Map, ESRI, Tomtom, Garmin, Foursquare, FAO, Meti/NASA, USGS) and train track data by OpenStreetMap (Humanitarian OpenStreetMap Team, 2024).*

South Africa (Figure 1). The Saldanha Bay Municipality hosts the Saldanha Bay port and the surrounding Besaansklip industrial area. The industrial area is surrounded by several residential areas, with Vredenburg and Saldanha being the most populated. The area is semi-arid, with a winter rainy season and an average annual rainfall of approximately 230 mm. The wind in this area is predominantly from the south to the southwest (Figure 2a and Figure 2b), but northern winds also prevail in winter, from April to September (Figure 2b). The weather conditions are explained in more detail in Vos et al. (2024).

Dust sampling and analyses

For this study, two monitoring datasets were used to quantify the potentially toxic metals in airborne dust. The first dataset originates from the Saldanha Bay Municipality's monitoring efforts conducted following the air monitoring guidelines stipulated in the National Framework for Air Quality Management (DEA, 2017). Dust buckets collected deposited particles, and from these samples, the concentrations of selected target metals, Fe, Mn, Cu, Zn, and Pb were measured. This monitoring was performed monthly at seven stations since 2014. For this study, we considered the dust deposition data from 2016 to 2023 due to data gaps in the earlier years. In total, 461 samples were taken. More details on this municipal monitoring are described in the *Dust monitoring 2016 to 2023* section. This long-term monitoring approach allows the determination of the temporal and spatial variability. However, the national air monitoring guidelines only prescribe the monitoring of the five metals (DEA, 2017), despite the larger number of potentially toxic metals associated with industrial, smelting, traffic, and mining processes.

Additional sampling was conducted to expand the array of metals to be included in the risk analyses. Five Big Spring Number Eight (BSNE) samplers, which capture the horizontal flux of dust, were installed in residential areas (Figure 1). The sampling period was from 18 September 2023 to 13 November 2023. The following suite of metals was determined in this additionally collected dust in 2023 and 2024: Al, As, Ba, Cd, Co, Cr, Cu, Fe, Mn, Mo, Ni, Pb, Sb, Se, Sn, Sr, V, and Zn. These metals were chosen due to their potential health impacts and their association with mining and industrial activities (Al-Swadi et al., 2022; Briffa et al., 2020; Chen et al., 2022; Csavina et al., 2012; Okanigbe et al., 2017; Ondrasek et al., 2025). This method is discussed more extensively in the *Extended dust sampling for additional relevant metals* section. By combining both approaches, we aim to understand the changes in metal content over time and the spatial variability, while simultaneously being able to evaluate the health risks of a wider range of potentially toxic metals.

Dust monitoring 2016 to 2023

The Municipality of Saldanha Bay has been monitoring the dust deposition and dust chemical content at seven sites using so-called 'dust buckets'. These monitoring stations are named north-A (N-A), north-B (N-B), northeast (NE), central north (CN), central south (CS), southwest (SW), and southeast (SE) according to their relative location within the sampler array (Figure 1). The dust was collected roughly once per month, but during and in the aftermath of the COVID-19 pandemic, the sampling intervals were longer. For each sampling period, the depositional flux (in mg day^{-1} m^{-2}) and the content of Fe, Mn, Cu, Zn, and Pb (in ppm) of the deposited dust were determined. The depositional flux

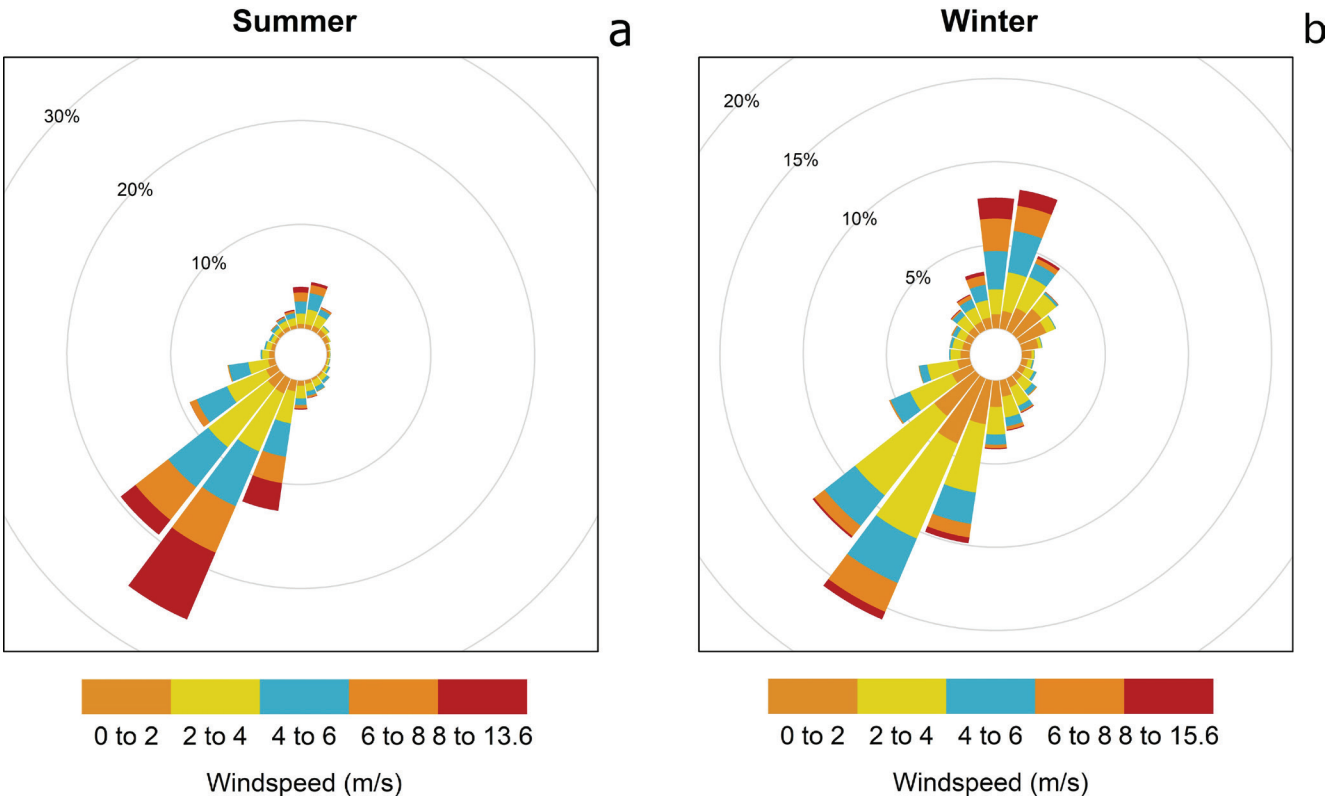

Figure 2: *Summertime (a) and wintertime (b) wind roses for the study area measured hourly from 2016 to 2023 at the climate station in Langebaanweg (Figure 1). Here, summer is considered to span from October to March, and winter from April to September.*

of the total dust was analysed by Vos et al. (2024). Combining the total deposition flux with the content of the dust, the deposition flux (in mg m^{-2} day^{-1}) of the specific elements can be calculated. The dust and metal content analysis was conducted in the Société Générale de Surveillance (SGS) Environmental Laboratory in Randburg, South Africa, a South African National Standards (SANS) 17025-accredited facility. The samples were digested with a mixture of nitric and hydrochloric acids, following National Institute for Occupational Safety and Health (NIOSH) methods 7300 and 7301 (NIOSH, 1994). The digest is then analysed by inductively coupled plasma optical emission spectrometry (ICP-OES). The dataset is publicly available at https://sbm.gov.za/environmental. Due to the long monitoring period and monthly measurement interval, it is possible to determine the long-term and seasonal variability of the metal fluxes and the variability between the different stations.

Extended dust sampling for additional relevant metals

To expand the number of metals included in the health risk assessment, five BSNEs were additionally installed, from which the sampled dust was analysed. These five BSNE samplers were installed at the stations named St Helena Bay, Vredenburg, Saldanha, Blouwater Bay, and Langebaan (Figure 1). These passive dust samplers captured the horizontally travelling particles. It should be noted that, similar to the dust buckets, the BSNEs are likely to capture the larger dust particles that are suspended in the atmosphere (Goossens, 2004; Mendez et al., 2016; Yang et al., 2018). In these five samples, the Al, As, Ba, Cd, Co, Cr, Mo, Ni, Sb, Se, Sn, Sr, and V content were analysed in addition to the Cu, Fe, Mn and Pb content that were also measured by the municipality (see *Dust monitoring 2016 to 2023*). The dust was analysed for the metal content with an Agilent 7900 Inductively Coupled Plasma Mass Spectrometry (ICP-MS) at Stellenbosch University Central Analytical Facilities (CAF) following digestion with nitric acid and hydrochloric acid using the MARS microwave digester vessels.

Data analyses

To determine the relationship between different values and the statistical significance between different groups, several statistical tests were used. To calculate whether two groups of datasets differ significantly from each other, Wilcoxon tests were done. To compare multiple groups of datasets, ANOVA tests were utilised. For both the Wilcoxon and ANOVA tests, an alpha value of 0.01 was used for statistical significance. When determining the seasonal patterns of dust fluxes, the values from summer (October to March) and winter (April to September) were compared. For the development and visualisation of the statistical analyses, the R packages “stats” (R Core Team, 2013) and “ggplot2” (Wickham, 2016) were used. To visualise the relationship between multiple units, such as metal concentrations, a correlation matrix was created using the package “corrplot” in R (Wei and Simko, 2021).

Health risk assessment

In this study, we focus on the possible toxic effects of metals in dust. The health risk assessment model from the United States Environmental Protection Agency (US EPA, 1996, 1989) estimates the carcinogenic and non-carcinogenic health risks of potentially toxic metals in dust particles. It should be noted that these health risk indices serve as an initial assessment of the possible risks of metals in dust and that they do not represent the measured health impacts in a given community.

Chemical daily intake

To determine the impact of toxic metals in dust, we calculated the Chemical Daily Intake of toxic metals (CDI, in mg kg^{-1} day^{-1}) via inhalation (CDI_{inh}), ingestion (CDI_{ing}), and dermal absorption through skin contact (CDI_{dermal}). The intake via ingestion is generally the highest of the three routes (Dahmardeh Behrooz et al., 2021; Drahota et al., 2018; Ma et al., 2022; Zheng et al., 2020), and is especially high for children (Guney et al., 2010). The CDI values were calculated with equations 1 to 3 (US EPA, 1989):

$$\mathrm{CDI_{inh}} = \mathrm{C_{ppm}} * \frac{\mathrm{R_{inh}} * \mathrm{F_{exp}} * \mathrm{T_{exp}}}{\mathrm{PEF} * \mathrm{ABW} * \mathrm{T_{avg}}} \quad (1)$$

$$\mathrm{CDI_{dermal}} = \mathrm{C_{ppm}} * \frac{\mathrm{SAF} * \mathrm{A}_{skin} * \mathrm{DAF} * F_{\mathrm{exp}} * \mathrm{T_{exp}}}{\mathrm{ABW} * \mathrm{T_{avg}}} * 10^{-6} \quad (2)$$

$$\mathrm{CDI_{ing}} = \mathrm{C_{ppm}} * \frac{\mathrm{R_{ing}} * \mathrm{F_{exp}} * \mathrm{T_{exp}}}{\mathrm{ABW} * \mathrm{T_{avg}}} * 10^{-6} \quad (3)$$

Where C_{ppm} represents the elemental concentration (in ppm), R_{inh} is the dust inhalation rate (in m^3 day^{-1}), Ring is the dust ingestion rate (in mg day^{-1}), F_{exp} is the exposure frequency (in day $year^{-1}$), T_{exp} is the time of exposure (in years), PEF is the particulate emission factor (in m^3 kg^{-1}), ABW is the average body weight (in kg), and T_{avg} is the average time of illness to develop (T_{exp} expressed in days), SAF is the skin adherence factor in mg cm^{-2} hr^{-1}, A_{skin} is the exposed skin area in cm^{-2}, and DAF is the dermal absorption factor. The values used for these calculations are shown in Table 1. For this model, we will differentiate between

Table 1: *The exposure parameters used to calculate the CDI using equations 1 to 3.*

Parameter	Adults	Child	Reference
R_{ing}	100 mg day^{-1}	200 mg day^{-1}	US EPA 1996; 2011
R_{inh}	20 m^3 day^{-1}	7.6 m^3 day^{-1}	Van den Berg 1994
F_{exp}	350 days $year^{-1}$	350 days $year^{-1}$	US EPA 1996
T_{exp}	24 years	6 years	US EPA 1996
PEF	1.36 * 109 m^3 kg^{-1}	1.36 * 109 m^3 kg^{-1}	US EPA 2001
ABW	70 kg	15 kg	US EPA 1989
T_{avg} non-carcinogenic	T_{exp} * 365 days	T_{exp} * 365 days	US EPA 1996
T_{avg} carcinogenic	25,550 days	25,550 days	US EPA 2001
SAF	0.70 mg cm^{-2} hr^{-1}	0.07 mg cm^{-2} hr^{-1}	US EPA 2001
A_{skin}	5700 cm^{-2}	2800 cm^{-2}	US EPA 2001
DAF	0.001	0.001	US EPA 2001

the effects on children and adults. It is important to note that the values used to calculate the CDI and represented in Table 1 are general assumptions on personal exposure (such as F_{exp} and T_{exp}) and body characteristics (such as BW and A_{skin}). For this reason, the calculated CDI does not represent exact individual intakes but rather a general estimation of the intake and the associated risks.

The concentration (C_{ppm}) reflects the 'reasonable maximum exposure' (US EPA, 1989). In the case of the monitoring data, this is defined as the 95% upper limit concentration (Hu et al., 2011; US EPA, 1996), which is calculated for the total dataset and each individual station. For the additional sampling, due to the limited number of samples, the maximum concentration measured is used to represent the reasonable maximum exposure.

Hazard Index and Carcinogenic Risk

From the CDIs, the non-carcinogenic Hazard Index and the Carcinogenic Risk per element are calculated using equations 4 and 5 (US EPA 1989, 1996, 2001):

$$\text{Hazard Index} = \sum \frac{\text{CDI}_{\text{inh,dermal,ing}}}{RfD_0} * \text{BAF} \quad (4)$$

$$\text{Carcinogenic Risk} = \sum \text{CDI}_{\text{inh,dermal,ing}} * \text{BAF} * \text{SF} \quad (5)$$

Here, RfD is the reference dose (mg kg^{-1} day^{-1}) and BAF is the bioaccessibility factor (%), see Table 2. For the elements that could have a carcinogenic impact via ingestion (As and Cr(VI)), the carcinogenic risk is calculated with the BAF and the slope factor (SF), which is an estimate of the increase in carcinogenic risk per element (mg kg^{-1} day^{-1}) (US EPA, 2011). The BAF can have a large variability depending on the dust and the intake pathways (Hu et al., 2011; Okorie et al., 2012), and it is not known for each element. When a BAF value is not presented in the literature, a bioaccessibility of 100% is assumed to represent the maximum risk that this metal poses. This assumption also means that the Hazard Index of this element might be overestimated. For the Hazard Index, a value above 1 indicates that there are significant non-carcinogenic health risks (US EPA 2001), where a higher Hazard Index represents a higher possible impact. A Hazard Index value below 1 means that the dust has a likely non-significant health effect. For the Carcinogenic Risk, a value below 1.0E-4 is considered tolerable (US EPA 2001). A detailed overview of the parameters and factors included in the Hazard Index and carcinogenic risk assessments is presented by the US EPA (2011).

Oxidation states of Cr and As

For the Hazard Index and related calculations, our analysis provided concentrations of total Cr and total As, which neglect speciation. However, the toxicity is species-dependent for both metals. Cr(VI) is much more soluble, mobile, and toxic than Cr(III), which is largely insoluble, immobile and less toxic. Cr in dust particles from eroded soil, including mine dust, typically occurs as Cr(III), such as in chromite; Cr(VI)-bearing minerals, in contrast, are rather rare. In the atmosphere, Cr typically exists as Cr(III)

Table 2: *Bioaccessibility factors (BAF), reference dose (RfD) values, and slope factors (SF) are used to calculate the Hazard Index and Carcinogenic Risk per element as described in equations 4 and 5. The BAF values are sourced from Hu et al. (2011), and the RfD and SF values are sourced from US EPA (2023) guidelines, except for the Pb values, which were provided by WHO (2017)*

Element	BAF (%)	RfD	SF
Al	-	1	-
As	38.8	3.0E-4	1.5
Ba	-	0.2	-
Cd	74.5	1.0E-4	-
Co	22.1	3.0E-4	-
Cr (VI)	5.83	3.0E-3	0.5
Cu	29.8	4.0E-2	-
Fe	3.88	0.7	-
Mn	47.6	2.4E-2	-
Mo	-	5.0E-3	-
Ni	15.7	1.1E-2	-
Pb	47.0	3.5E-3	-
Sb	-	4.0E-4	-
Se	-	3.0E-3	-
Sn	-	0.6	-
Sr	-	0.6	-
V	11.2	5.0E-3	-
Zn	60.1	0.3	-

(Torkmahalleh et al., 2013), particularly in particles derived from soil erosion, mainly because the oxidation from Cr(III) to Cr(VI) is slow in the atmosphere and limited to a few constituents such as ozone or Mn dioxide (Stanin, 2005). However, the oxidation of Cr(III) to Cr(VI) in the natural environment may occur whenever conditions are favourable (Apte et al., 2006). Bell and Hipfner (1997) reported that Cr(VI) contributed approximately 20% to the airborne Cr in a small urban area in Canada. Also, Cr(VI) has been reported as enriched in $PM_{2.5}$ (Yu et al., 2014) and found to contribute up to 50% of the total Cr in city centres and around 30–40% in aerosols collected close to road traffic (e.g., Świetlik et al., 2011). Consequently, in our health risk estimates, we use a Cr(VI) contribution to a total measured Cr of 25%, following Keshavarzi et al. (2015) and Soleimani-Sardo et al. (2023).

Trivalent arsenic (As(III)) is much more toxic to humans than pentavalent arsenate (As(V)). In atmospheric particulate matter, As(V) is the dominant (50-99%) inorganic form in urban (Huang et al., 2014; Lin et al., 2022; Tanda et al., 2020), industrial (Sánchez-Rodas et al., 2007) and remote (González-Castanedo et al., 2015) areas around the world. Nonetheless, it appears that at least in urban areas, As(III) increases in the fine PM (Huang et al., 2014; Nocoń and Rogula-Kozłowska, 2019), and As(III) can be the dominant species in $PM_{2.5}$ (Tirez et al., 2015). Here, we follow the EPA guidelines using total As in our health risk

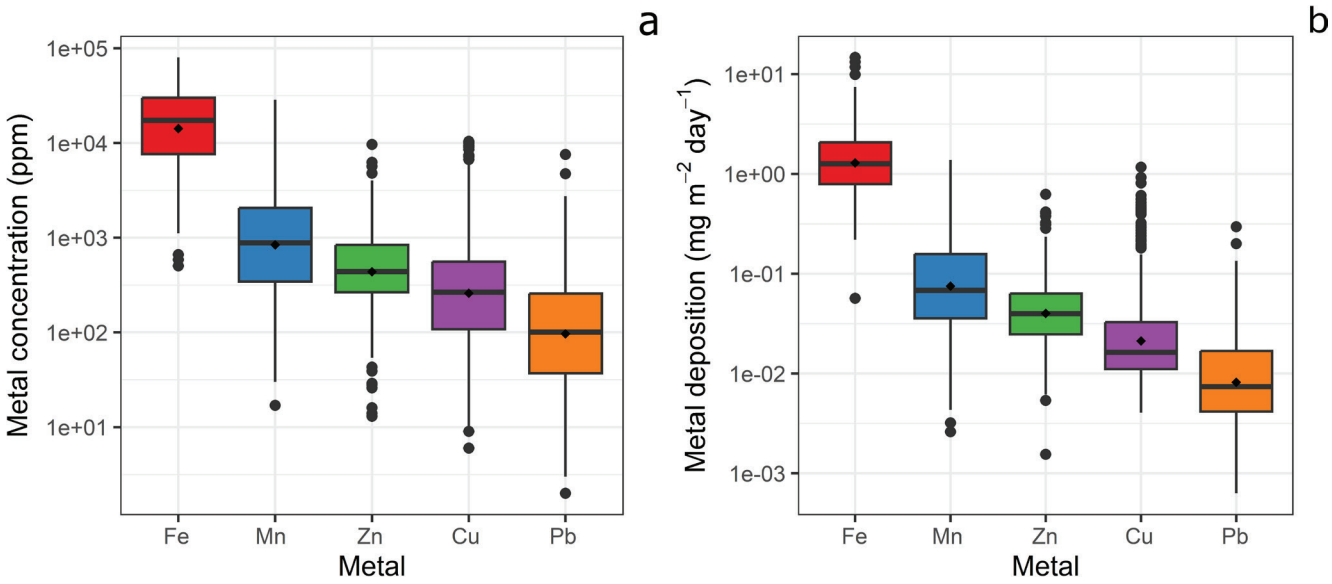

Figure 3: *The concentration of the metals Fe, Mn, Zn, Cu, and Pb (a), and the metal deposition flux (b), measured from 2016 to 2023, at the seven monitoring stations as shown in Figure 1. The boxplot displays the distribution of the dataset: the box spans the interquartile range (Q1 to Q3) with a line marking the median (Q2). Whiskers extend to the lowest and highest values within 1.5 × IQR, while values outside this range appear as points. A diamond indicates the dataset's mean.*

calculations, considering that most of the total As is pentavalent. Nevertheless, the resultant Hazard Index might underestimate the actual risk in areas where dust is predominantly fine PM and contains non-negligible contributions of As(III).

Results

Dust composition and deposition flux

During the monitoring of the dust deposition at seven stations from 2016 to 2023 (see Figure 1), the concentrations of the potentially toxic metals Fe, Mn, Zn, Cu, and Pb in the dust were measured (Figure 3a). For these metals, the variance of the concentration is between 100 to 1000-fold. By combining the dust composition and the total dust deposition flux, the metal deposition flux was calculated (Figure 3b), which shows a similarly large variance. Despite this large variance, some patterns are distinguishable: Fe showed the highest concentrations and fluxes, whereas lower concentrations and fluxes were observed for Mn, Zn, and Cu. The lowest concentrations and fluxes were observed for Pb (Figure 3).

The Fe, Mn, Zn, Cu, and Pb concentrations in the dust show a generally moderate positive relationship with each other ($r > 0.44$; Figure 4). In contrast, each individual metal concentration is strongly negatively correlated to the total dust deposition flux ($r < -0.62$, $p < 1.0E-15$; Figure 4). This indicates that a high dust deposition flux is mainly influenced by particles with low Fe, Mn, Zn, Cu, and Pb contents. Furthermore, each metal flux correlates significantly but weakly to the total dust deposition flux ($r = -0.08$, 0.11, 0.33, 0.28, and 0.14, and $p = 0.0063$, 0.013, 0.0022, 3.81E-13, and 5.6E-10 for Pb, Cu, Mn, Zn, and Fe, respectively; Figure 4). The negative correlation between the total dust flux and each metal concentration of the dust, and

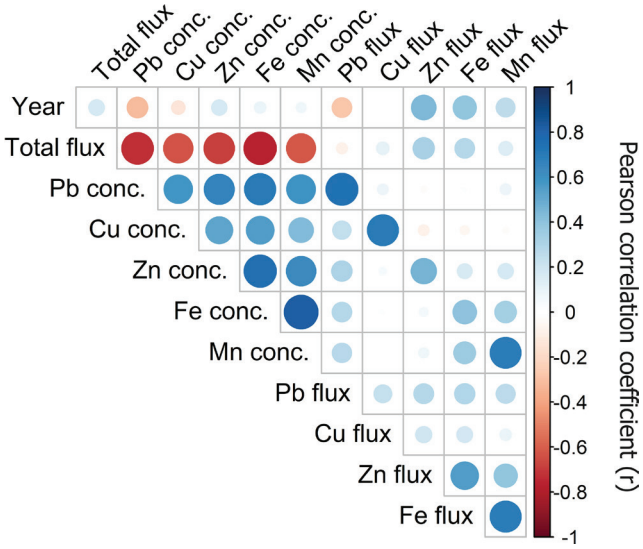

Figure 4: *Correlation matrix showing the relationships between the year of sampling and the logarithmic value of the total dust deposition flux, the metal concentration, and the metal dust deposition flux.*

the weak correlation between the total dust flux and each metal flux, emphasise that the total dust deposition should not be regarded as representative of the metal quantity in dust. In contrast, the metal concentrations correlate strongly with the respective metal fluxes for Pb, Cu, and Mn ($r > 0.69$, $p < 1.0E-15$), and moderately for Fe and Zn ($r = 0.41$ and 0.46, respectively, and $p < 1.0E-15$; Figure 4). This indicates that the concentration of a metal is a good indicator of the flux of this same metal, but that these values should not be considered interchangeable. In contrast to the good correlation among metal concentrations, only a few of the fluxes of different metals correlate well, such as the Fe and Mn flux or the Fe and Zn flux (Figure 4).

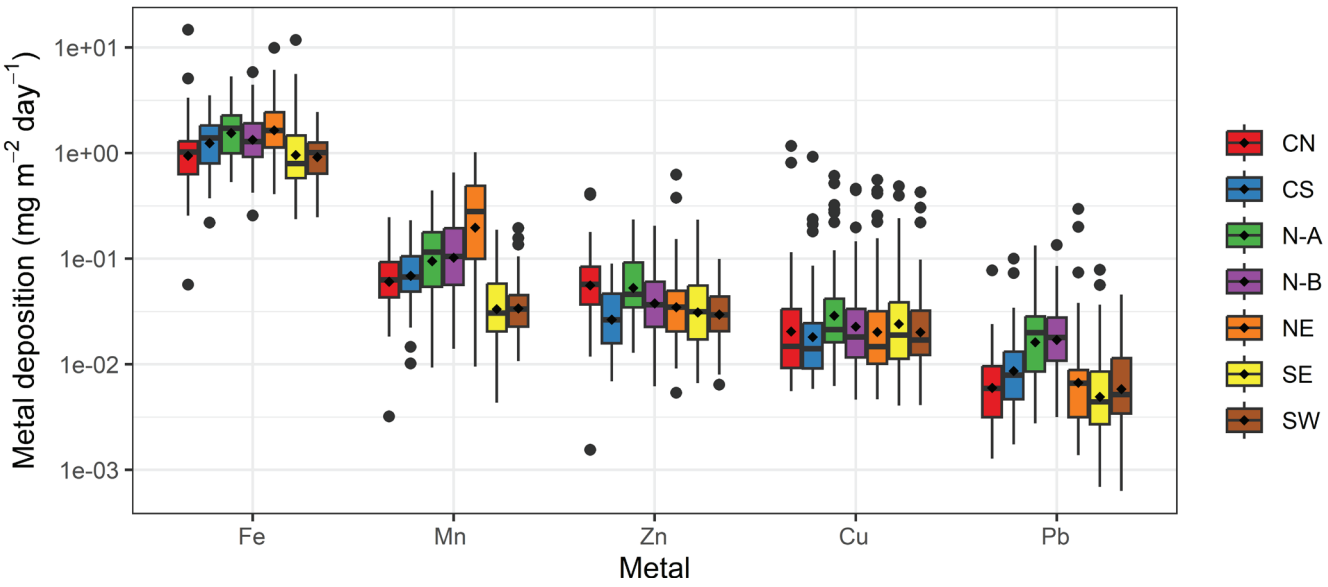

Figure 5: *The elemental deposition of Fe, Mn, Zn, Cu, and Pb measured from 2016 to 2023 at the different monitoring stations from the municipality, grouped per monitoring station. See Figure 1 for the location of the monitoring stations. The boxplot displays the distribution of the dataset: the box spans the interquartile range (Q1 to Q3) with a line marking the median (Q2). Whiskers extend to the lowest and highest values within 1.5 × IQR, while values outside this range appear as points. A diamond indicates the dataset's mean.*

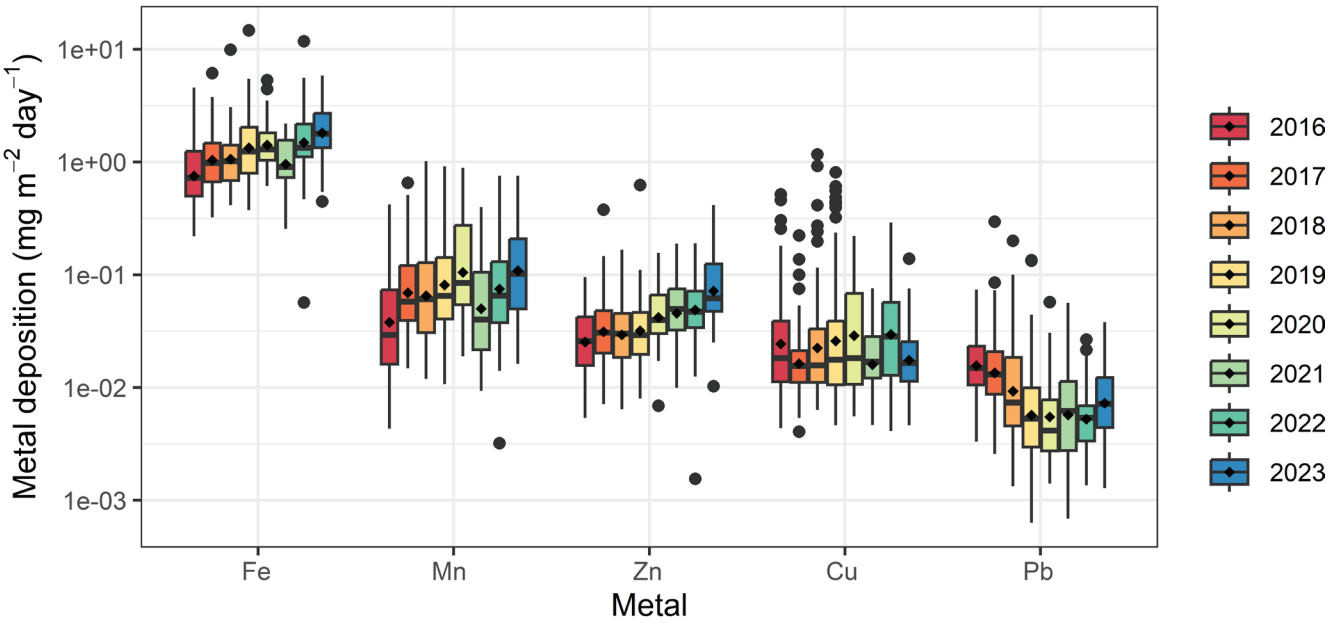

Figure 6: *The metal deposition flux measured from 2016 to 2023 at the municipal monitoring stations, grouped per year. The boxplot displays the distribution of the dataset: the box spans the interquartile range (Q1 to Q3) with a line marking the median (Q2). Whiskers extend to the lowest and highest values within 1.5 × IQR, while values outside this range appear as points. A diamond indicates the dataset's mean.*

Spatial variability of metal fluxes

The individual metal fluxes seem to be generally similar between the seven investigated stations across the industrial hub and its surroundings (Figure 5). ANOVA analyses served to test for significant changes in the metal fluxes between different monitoring sites (See Supplementary 1). The only metal that does not show any statistically significant difference in the depositional flux per station is Cu. The stations that have statistically similar metal fluxes are the close-lying N-A and N-B, and the southern stations SW, CS, and SE. There is a generally higher flux of Mn, Fe, Zn, and Pb in the northern sites N-A, N-B, and NE, but the exact flux pattern varies for each metal. The high metal flux in this northern area could be the result of the winds from the south crossing the industrial area on the way north.

Temporal variation of the metal fluxes

To determine the annual variation in the deposition fluxes of Fe, Mn, Zn, Pb, and Cu, the fluxes of each metal are grouped per year (Figure 6). The ANOVA analyses of these fluxes between the different years are shown in Supplementary 2 and show only limited changes between the years. However, the Pearson correlation coefficients (Figure 4) indicate a weak positive correlation between the years and the deposition flux of Zn ($r = 0.44$, $p < 1.0E\text{-}15$), Fe ($r = 0.39$, $p < 1.0E\text{-}15$), and Mn ($r = 0.25$,

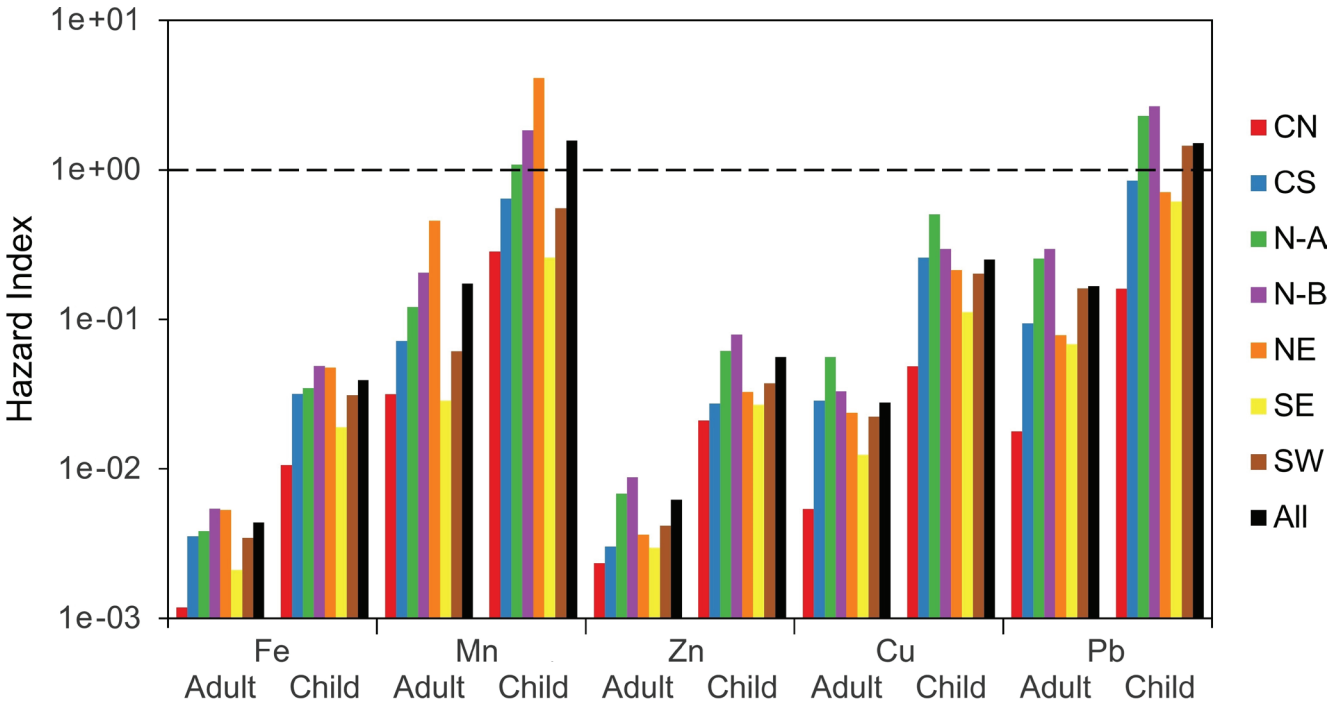

Figure 7: *The Hazard Index calculated from data from 2016 to 2023 for the seven monitoring stations and the total, for children and adults. These values are based on the intake and conditions described in Table 1 and Table 2, and equations 1 to 5. See Figure 1 for the location of the monitoring stations.*

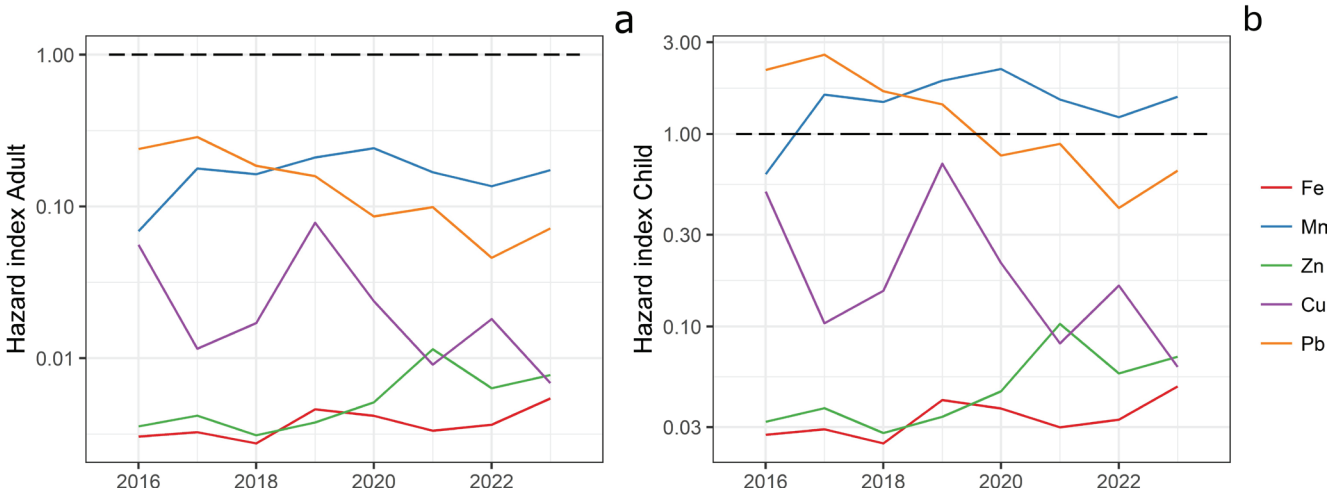

Figure 8: *The annual Hazard Index of Fe, Mn, Zn, Cu, and Pb from 2016 to 2023 for adults (a) and children (b). This is measured from the seven monitoring stations. The annual Hazard Indices are based on the yearly dust conditions, the intake and conditions described in Table 1 and Table 2, and equations 1 to 5. Note the logarithmic y-axis scale.*

p = 1.5E-8). Figure 6 visualises this increase in these fluxes over the years. The Pb flux, in contrast, shows a general decrease in deposition flux (r = -0.28, p = 8.7E-10), which is especially noticeable between 2016 and 2020. In addition to the interannual changes, Wilcoxon tests revealed a few seasonal differences (Supplementary 3, Table 3). The Fe, Mn, and Pb fluxes show a seasonal pattern at certain sites, especially at the stations north of the industrial area. Generally, higher fluxes were observed in summer, arguably caused by more prominent southern winds in summer (Figure 2 and Vos et al. 2024). The differences in both seasonal and annual variations of metal fluxes indicate the diversity of sources and behaviours of metals in aerosols.

Table 3: *Summary of the statistically significant differences observed between the deposition flux for different metals in summer and winter at different stations. The full analyses are shown in Supplementary 3. See Figure 1 for the location of the monitoring stations.*

Deposition flux	Seasonal higher flux
Total flux	N-A, SW (summer), NE (winter)
Pb	N-A, N-B (summer)
Fe	N-A, N-B, NE, SW (summer)
Mn	N-B, NE (summer), SW (winter)
Cu	None
Zn	None

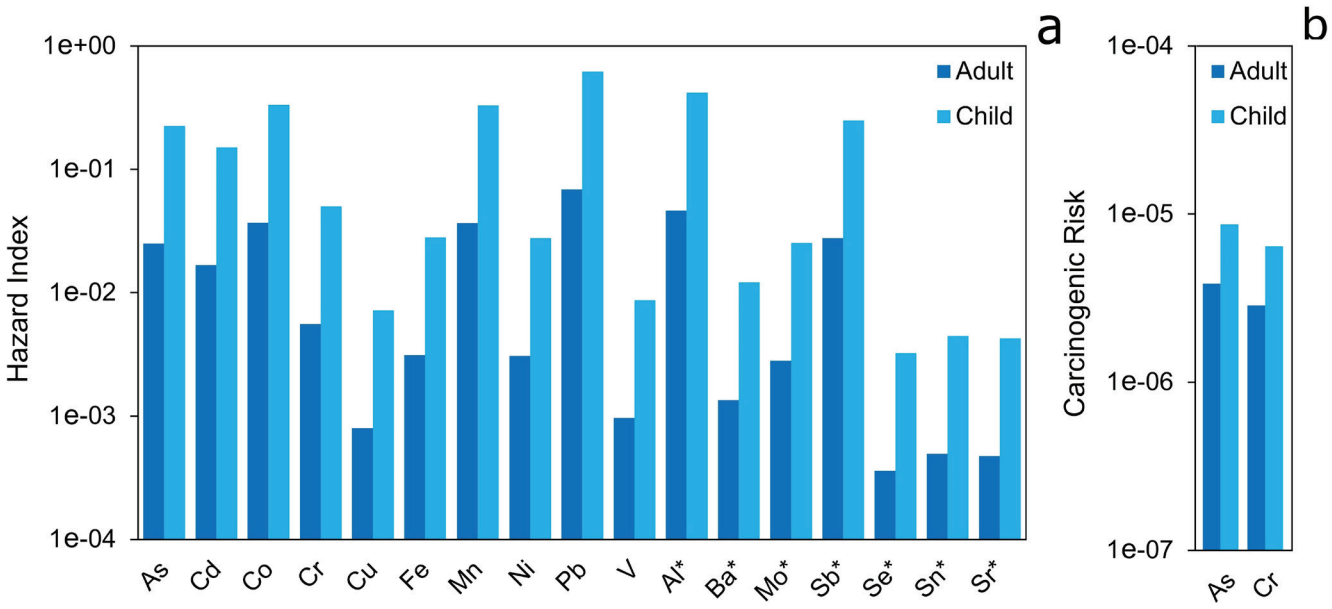

Figure 9: *The Hazard Index (a) and Carcinogenic Risk (b) calculated for children and adults from the five BSNE samples as described in section 2.4. BSNE sampler stations are given in Figure 1. The Hazard Index and Carcinogenic Risk values are based on the intake and conditions described in Table 1 and Table 2, and equations 1 to 5. Elements marked with an asterisk have no known BAF, and the assumed 100% BAF might lead to an overestimated Hazard Index.*

Hazard indication of dust exposure based on toxic metal content

The CDI via the three main exposure pathways (inhalation, ingestion, and dermal contact) was calculated using the measured metal concentrations (equations 1 to 3, see the *Health risk assessment* section). The different CDIs (see Supplementary 4) indicate that ingestion is the predominant intake route, followed by inhalation and dermal contact, which is consistent with findings from previous studies (Kurt-Karakus, 2012; Li et al., 2022; Mohmand et al., 2015). The CDI is furthermore higher for children, which can be linked to their lower body weight and higher presumed ingestion rate. From the total CDI, the Hazard Index was determined (Figure 7). The Hazard Indices were elevated for children due to higher CDI values. The non-carcinogenic Hazard Indices rank in the order of Mn > Pb > Cu > Zn > Fe (Figure 7). The Hazard Index calculated from all stations exceeds the threshold value of 1 for Mn and Pb, indicating that there may be significant health risks, especially at certain stations (Figure 7). The Mn Hazard Index exceeds the threshold at the northern stations N-A, N-B, and NE, while the Pb Hazard Index exceeds the threshold value at stations N-A, N-B, and SW.

Overall, the metal deposition fluxes increased for Fe, Mn, and Zn from 2016 to 2023, but decreased for Pb (Figure 4 and Figure 6). A similar temporal pattern can be seen in the Hazard Index of these elements calculated from all stations (Figure 8). As such, the increasing Mn content over time led to a Hazard Index higher than 1 since 2017, whereas the decline in Pb resulted in acceptable Hazard Index values since 2019, although an increase in the Hazard Index value is noted with the increase in Pb concentration in 2023. Figure 8 also illustrates strong fluctuations over time, as observed, for example, in the Cu Hazard Index. These fluctuations highlight the importance of multi-year monitoring over snapshot testing. It should furthermore be noted that the Hazard Index is not a definite assessment of the health impact, and a value below one does not represent an exclusion of any possible health impacts.

While the municipal long-term monitoring targeted a selected few metals, an extended suite of potentially toxic metals was measured in dust collected using the BSNE samplers in 2023 (see the *Dust sampling and analyses* and *Extended dust sampling for additional relevant metals* sections). The metal concentrations from the individual station are in Supplementary 5, and the calculated CDI values are reported in Supplementary 6. This extended suite allows calculating Hazard Indices and Carcinogenic Risk of potentially toxic metals (Figure 9). Again, the risk is higher for children, who have a generally higher CDI than adults. Neither the Hazard Indices nor the Carcinogenic Risk exceeded the threshold of 1 and 1.0E-4, respectively. However, similar to the monitoring data, certain elements such as Al, As, Cd, Co, Mn, Pb, and Sb do approach the threshold of the non-carcinogenic Hazard Index. It should be noted that for several elements, including Al and Sb, the BAF value was not known and was set to 100%, possibly leading to overestimates of the Hazard Index value of these elements.

Discussion and conclusion

Comparison with other urban and industrialised areas

The potentially toxic metal content in the residential areas around the industrial hub of this study was compared to previously published contents in other urban areas around the world (Table 4). For this comparison, average values of

previously published metal content in urban dust were used. We selected studies spanning a similar time period, i.e. the last 10 years, that investigate the potentially toxic metals in outdoor dust in residential and urban areas (Table 4). Some are located near industrial areas, but we did not include studies directly measuring industrial emissions. The elements Ba, Mo, Sb, Se, Sn, and Sr were excluded since these were rarely measured in dust content studies. This comparative study is not exhaustive, and it solely serves to illustrate the variability of metal content that can be found in and around urban areas, often under industrial impact and provide context for the interpretation of our findings.

Several of the metal contents (in ppm) measured around Saldanha Bay are higher (e.g., Mn, Co, Cu, and Ni) than in other urban areas of the world (Table 4). The average Mn content in our study is the highest of all reported concentrations. The average Co content from this study is only lower than that measured in Akure, Nigeria (Adewumi, 2022). Similarly, the average Cu content is only lower than that measured in Antofagasta in Chile, which hosts a copper concentrate stockpile (Tapia et al., 2018). The Ni content is only lower than that measured in Dezful, Iran (Mostafaii et al. 2021). Lastly, Cr and Pb contents are higher than in most of the other urban studies. The Cd, Fe, and

Table 4: *The average metal content of dust (in ppm) in urban areas presented in recent studies around the world. Referenced studies were selected as focusing on a similar time period, i.e. the last 10 years and investigating similar potentially toxic metals in outdoor dust in residential and urban areas. n – indicates the number of samples included in the respective study.*

		Mean concentration (ppm)										
Study	**n**	**Fe**	**Mn**	**Cu**	**Zn**	**Pb**	**As**	**Cd**	**Co**	**Cr**	**Ni**	**Place**
This study	451-461	20865	1808	685	691	245						Saldanha Bay Municipality, South Africa - Monitoring
This study	5						5	0.7	25	434	118	Saldanha Bay Municipality, South Africa - Additional sampling
Mvovo and Magagula (2022)	54		316		161	89		0.2			23	East London, South Africa
Delibašić et al. (2020)	117	3150	236	30	82	52		3.2		33	73	Towns of Bosnia and Herzegovina
Safiur Rahman et al. (2019)	88		262	50	239	19	8.1	11.6		144	37	Dhaka, Bangladesh
Tapia et al. (2018)	31	39564	537	10821	11869	710	239.4	45.0	17	61	29	Antofagasta, Chile
Li et al. (2022)	9	33624	668	71	1425	1841	22.7	1.7	13	203	31	Ebinur Lake Basin, China
Wang et al. (2020)	7			119	803	251		0.9		492		Panzhihua, China - Industrial area
Wang et al. (2020)	7			147	795	214		0.8		538		Panzhihua, China - Heavy traffic areas
Wang et al. (2020)	6			139	789	209		0.8		490		Panzhihua, China - Residential area
Zhaoyong et al. (2019)	34		829	140	792	147	44.0	3.1	19	279	43	58 Chinese cities
Jadoon et al. (2021)	13		251	80	169	70		0.3	3	24	14	Alexandria, Egypt
Jadoon et al. (2021)	10		343	37	192	30		0.2	7	32	20	Kafr El-Sheikh, Egypt
Rani et al. (2019)	12				220	195			22	200	56	Kharagpur Town, India
Dehghani et al. (2017)	30		864	275	666	213	5.4	0.8		77	58	Teheran, Iran
Mostafaii et al. (2021)	5	29035				45		1.3		394	320	Dezful City, Iran
Alsbou and Al-Khashman (2017)	55	4694		12	25	32		9.7				Petra region, Jordan
Aguilera et al. (2021)	482	5722	235	100	281	128			7	51	36	Mexico City, Mexico
Batbold et al. (2021)	57			66	571	52	16.5		10	70	21	Ulaanbaatar, Mongolia
Adewumi (2022)	16	115		38	73	32	1.8	3.0	39	3	12	Akure City, Nigeria
Mohmand et al. (2015)	10		77	61	124	189		1.2	2	15	7	Punjab, Pakistan - Industrial
Mohmand et al. (2015)	10		93	13	196	170		2.3	3	20	8	Punjab, Pakistan - Urban
Mohmand et al. (2015)	10		90	12	137	62		0.4	2	6	5	Punjab, Pakistan - Rural
Trojanowska and Świetlik (2020)	4	20600	565	239	618	88				54	50	Radom, Poland
Al-Swadi et al. (2022)	3	18500	357	127	982	39		0.7	8	30	29	Mahad AD'Dahab, Saudi Arabia - Urban
Al-Swadi et al. (2022)	2	15000	294	24	666	7		0.1	5	19	20	Mahad AD'Dahab, Saudi Arabia - Suburban
Al-Swadi et al. (2022)	17	12900	210	24	599	16		0.1	5	30	27	Riyadh, Saudi Arabia - Urban
Al-Swadi et al. (2022)	2	11500	179	10	603	9		0.0	3	24	22	Riyadh, Saudi Arabia - Suburban
Delgado-Iniesta et al. (2022)	35			411	895	290		1.3		100	42	Madrid, Spain
Rakhmatov and Abdullaev (2021)	104			56	1056	61	18.2		10	96	41	Sogd region, Tajikistan
Dat et al. (2021)	25		394	154	466	50		0.5	8	102	36	Ho Chi Minh City, Vietnam

Zn content, in contrast, are comparable to other urban studies, which is especially surprising for the Fe content considering the proximity to open-air Fe ore storage in the Saldanha Bay area. In summary, this global comparison shows that the metal content around this South African industrial hub can be considered high compared to other areas, with especially Mn, Co, Cr, Cu, Pb, and Ni being notable.

Variation of fluxes and composition

The dust at the seven monitoring stations reveals a large variation in the concentrations and fluxes of the potentially toxic metals Fe, Mn, Zn, Pb, and Cu (Figure 3). The total dust flux correlates negatively with the metal concentrations and shows a weak relationship with the metal dust fluxes. The total dust deposition flux should therefore not be considered representative of the quantity of potentially toxic metals. Partially, this negative or weak correlation between total dust flux and metal content might be explained by the grain size distribution. The particles with a low metal content are likely of natural origin and are of large grain sizes, such as sand and silt particles. Potentially toxic metals in dust are mainly associated with small particles such as $PM_{2.5}$ (Barcan, 2002; Csavina et al., 2012, 2011). Considering that such fine particles can penetrate the respiratory system, these particles would be more harmful to human health than larger particles like PM_{10}.

Distinct variation in the temporal and spatial patterns of the metal deposition fluxes suggests different sources of such elements and/or different behaviour of these elements as aerosols. Over time, a slow increase in dust deposition flux of Fe, Mn, and Zn, and a decrease in Pb have been observed since 2016. The increase in Fe, Mn, and Zn flux is likely caused by the general increase in industrial activities (AEC, 2022; DEA&DP, 2019). Pb in aerosol has mainly been associated with transport, mining, and smelting activities (Benin et al., 1999; Landrigan et al., 1975; Meza-Figueroa et al., 2009; Soto-Jiménez and Flegal, 2011). The closure of the Saldanha Steel smelting plant in 2020 could be associated with this decrease in Pb. Pb has furthermore been associated with traffic, and despite the phasing out of leaded gasoline since 2006 in South Africa, Pb concentrations in soils are still elevated around petrol stations (Mathee, 2014; Olowoyo et al., 2022). Hence, the observed trend in the Pb flux may reflect the effect of global and local policies challenged by legacy pollution and local sources. The fact that the elements show different changes over time shows that the main sources of these metals are likely different.

The Mn, Fe, and Pb deposition fluxes are higher in northern-lying stations. These elements also show a significantly higher deposition flux during summer. These high fluxes of Mn, Fe, and Pb at the northern stations could be caused by the dominating southern winds during summer, which transport more particles from the industrial area to the north. However, this would not explain the lack of a seasonal pattern at station SE, which would receive a higher flux in winter due to the more frequently occurring northern winds during this period. The seasonal patterns could furthermore be related to a change in industrial activities, so the exact cause of this spatial and seasonal variability cannot be determined with certainty. It does indicate, however, that monitoring efforts should take seasonal and spatial variability into account when determining potential risks in residential areas. Furthermore, Cu and Zn fluxes did not show a seasonal pattern, which again indicates the variability of the sources and emission of metals in this area.

Health risk assessment

To understand the possible health risks associated with the metals in the dust particles collected around the industrial hub of Saldanha Bay, the CDI for children and adults was calculated, from which the Hazard Index and Carcinogenic Risk could be derived. The CDI (expressed as mg kg^{-1} day^{-1}) is higher for children, which leads to a higher Hazard Index and Carcinogenic Risk for children. Considering the concentrations of Fe, Mn, Zn, Cu, and Pb from 2016 to 2023, the Hazard Index of Mn and Pb indicates potential risks for public health. Here, it should be noted that the Mn content has increased over time and could pose a more severe risk in the future. The additional sampling with the BSNEs to measure the Al, As, Ba, Cd, Co, Cr, Mo, Ni, Sb, Se, Sn, Sr, and V concentrations showed no significant risks of these metals. However, the Hazard Index values for children are above 0.1 for Al, As, Cd, Co, and Sb approach the threshold for a significant health risk. These metals may likely be related to industrial processes, mining, and/or traffic, due to the proximity to the industrial area and studies describing the common origin of the metals in aerosols (Csavina et al., 2012; Kar et al., 2010; Sánchez-Rodas et al., 2007). However, the exact origin of these metals in the Saldanha Bay Municipality has still to be determined. It should be noted that these values were only measured during one monitoring period and therefore only represent the metal concentration in dust during a short period of time. Public concern arose from visible dust deposition in the area. Despite the high visibility of the red dust emitted from Fe ore transporting, the measured Fe content of dust has a lower health risk than that of other elements due to the relatively high reference dose. Hence, visibility and health risks are not directly related.

Considering the enrichment in toxic metals and related possible significant non-carcinogenic risks, efforts to understand the behaviour of these metals are necessary. Future monitoring efforts could include a broader suite of metals, such as Al, As, Cd, Co, Cr, Ni, and Sb. By expanding the metals analysed, the risk assessment of potentially toxic metals and the change of these risks over time could be better addressed. Future studies should try to understand the precise origins of high-risk metals, whereby the focus could be on the Al, As, Cd, Co, Mn, Ni, Pb, and Sb. This could be the first step in developing mitigation strategies to limit the health impact of toxic metals in residential areas.

Critical evaluation of the health risk assessment

As previously mentioned, the CDI calculations are based on several generalised assumptions. To enhance the accuracy of

these assumptions, actual measurements of resident exposure to dust and toxic metals are needed, along with more detailed population data such as age, body weight, and inhalation rates. This should also include the sampling of metals using active samplers to address the concentration of airborne metals. This way, the health risks via inhalation can be better addressed. Additionally, incorporating active sampling methods to measure airborne metal concentrations would provide a clearer understanding of inhalation-related health risks. Furthermore, the BAF used to assess health risks varies considerably across studies, with a reported coefficient of variation ranging from 0.14 to 0.58 (Hu et al., 2011). Different studies also report differing BAF values (Hu et al., 2011; Okorie et al., 2012), which introduces uncertainty into risk assessments, as BAF values directly influence the calculated Hazard Index and Carcinogenic Risk. For some elements, such as Al and Sb, the absence of established BAF values may lead to an overestimation of associated health risks. In addition, as described in the *Health risk assessment* section, Cr and As exist in multiple oxidation states with considerably different toxicities. In this study, we assumed that Cr(VI) accounts for 25% of the total Cr content. However, given the high toxicity of Cr(VI) and the relatively high Hazard Index and Carcinogenic Risk of Cr in this region, determining the specific Cr(VI) content would be valuable. Likewise, As(III) is more toxic than As(V), and a more detailed analysis of arsenic speciation could enhance our understanding of the potential health impacts. In the future, studies evaluating public health and non-communicable diseases in this area should help to understand the risks, both general and carcinogenic, associated with the dust's geochemical composition in residential areas around such vital industrial hubs.

Recommendations

In areas where metal contents are high, albeit not yet leading to a clear indication of immediate health risks, future developments should be monitored carefully. Particularly, where strong, diverse industrial development and related traffic are co-located with formal and informal residential areas, regular spatially resolved metal content monitoring is advised. Furthermore, potential seasonal shifts in emission sources and particle transportation pathways should be considered. In addition, larger suites of metals rather than a selected few metals should be monitored, at least at a low temporal and spatial resolution to acknowledge the shifts in metal emissions with industrial development and transport pathways. Lastly, we recommend that metal speciation is included regularly in future monitoring efforts.

Statements and declarations

Acknowledgements

This work is based on the research supported in part by the National Research Foundation of South Africa (Grant Numbers CPRR150612119375, SRUG2204204036) awarded to Susanne Fietz. Funding for Heleen C. Vos was provided by the Department of Science and Innovation-funded Biogeochemistry Research Infrastructure Platform (BIOGRIP). The datasets generated during the current study are available in the Saldanha Bay Municipality repository: https://sbm.gov.za/environmental.

Author contributions

H.C. Vos and S. Fietz designed and conceptualised the study and were responsible for the project administration. I. Kangueehi and R. Toesie supported the logistical and methodological design. Sampling and sample analyses were performed by H.C. Vos, I. Kangueehi, and G. Ravenscroft. Data curation and formal analysis were performed by H.C. Vos. S. Fietz and R. Toesie acquired the funding. The first draft of the manuscript was written by Heleen C. Vos, and all authors contributed to the writing, editing and reviewing process. All authors read and approved the final manuscript.

References

Adewumi, A.J., 2022. Heavy Metals in Soils and Road Dust in Akure City, Southwest Nigeria: Pollution, Sources, and Ecological and Health Risks. Exposure and Health 14, 375–392. https://doi.org/10.1007/s12403-021-00456-y

AEC, 2022. The State of Saldanha Bay and Langebaan Lagoon 2021/2022 (Technical Report September 2022). Anchor Environmental Consultants, Cape Town.

Aguilera, A., Bautista, F., Gutiérrez-Ruiz, M., Ceniceros-Gómez, A.E., Cejudo, R., Goguitchaichvili, A., 2021. Heavy metal pollution of street dust in the largest city of Mexico, sources and health risk assessment. Environmental Monitoring and Assessment 193, 193. https://doi.org/10.1007/s10661-021-08993-4

Alsbou, E.M.E., Al-Khashman, O.A., 2017. Heavy metal concentrations in roadside soil and street dust from Petra region, Jordan. Environmental Monitoring and Assessment 190, 48. https://doi.org/10.1007/s10661-017-6409-1

Al-Swadi, H.A., Usman, A.R.A., Al-Farraj, A.S., Al-Wabel, M.I., Ahmad, M., Al-Faraj, A., 2022. Sources, toxicity potential, and human health risk assessment of heavy metals-laden soil and dust of urban and suburban areas as affected by industrial and mining activities. Scientific Reports 12, 8972. https://doi.org/10.1038/s41598-022-12345-8

Apte, A.D., Tare, V., Bose, P., 2006. Extent of oxidation of Cr(III) to Cr(VI) under various conditions pertaining to natural environment. Journal of Hazardous Materials 128, 164–174. https://doi.org/10.1016/j.jhazmat.2005.07.057

Barcan, V., 2002. Nature and origin of multicomponent aerial emissions of the copper–nickel smelter complex. Environment International 28, 451–456. https://doi.org/10.1016/S0160-4120(02)00064-8

Batbold, C., Chonokhuu, S., Buuveijargal, K., Gankhuyag, K., 2021. Source apportionment and spatial distribution of heavy

metals in atmospheric settled dust of Ulaanbaatar, Mongolia. Environmental Science and Pollution Research 28, 45474–45485. https://doi.org/10.1007/s11356-021-13861-2

Bell, R., Hipfner, J., 1997. Airborne Hexavalent Chromium in Southwestern Ontario. Journal of the Air & Waste Management Association (1995) 47, 905–10. https://doi.org/10.1080/10473289.1997.10464454

Benin, A.L., Sargent, J.D., Dalton, M., Roda, S., 1999. High concentrations of heavy metals in neighborhoods near ore smelters in northern Mexico. Environmental Health Perspectives 107, 279–284.

Briffa, J., Sinagra, E., Blundell, R., 2020. Heavy metal pollution in the environment and their toxicological effects on humans. Heliyon 6, e04691. https://doi.org/10.1016/j.heliyon.2020.e04691

Chen, L., Zhou, M., Wang, J., Zhang, Z., Duan, C., Wang, X., Zhao, S., Bai, X., Li, Zhijie, Li, Zimin, Fang, L., 2022. A global meta-analysis of heavy metal(loid)s pollution in soils near copper mines: Evaluation of pollution level and probabilistic health risks. Science of The Total Environment 835, 155441. https://doi.org/10.1016/j.scitotenv.2022.155441

Csavina, J., Field, J., Taylor, M., Gao, S., Landázuri, A., Betterton, E., Sáez, A., 2012. A Review on the Importance of Metals and Metalloids in Atmospheric Dust and Aerosol from Mining Operations. The Science of the total environment 433, 58–73. https://doi.org/10.1016/j.scitotenv.2012.06.013

Csavina, J., Landázuri, A., Wonaschütz, A., Rine, K., Rheinheimer, P., Barbaris, B., Conant, W., Sáez, A., Betterton, E., 2011. Metal and Metalloid Contaminants in Atmospheric Aerosols from Mining Operations. Water, air, and soil pollution 221, 145–157. https://doi.org/10.1007/s11270-011-0777-x

Dahmardeh Behrooz, R., Kaskaoutis, D.G., Grivas, G., Mihalopoulos, N., 2021. Human health risk assessment for toxic elements in the extreme ambient dust conditions observed in Sistan, Iran. Chemosphere 262, 127835. https://doi.org/10.1016/j.chemosphere.2020.127835

Dat, N.D., Nguyen, V.-T., Vo, T.-D.-H., Bui, X.-T., Bui, M.-H., Nguyen, L.S.P., Nguyen, X.-C., Tran, A.T.-K., Nguyen, T.-T.-A., Ju, Y.-R., Huynh, T.-M.-T., Nguyen, D.-H., Bui, H.-N., Lin, C., 2021. Contamination, source attribution, and potential health risks of heavy metals in street dust of a metropolitan area in Southern Vietnam. Environmental Science and Pollution Research 28, 50405–50419. https://doi.org/10.1007/s11356-021-14246-1

DEA, 2017. The 2017 National Framework for Air Quality Management in the Republic of South Africa. Department Of Environmental Affairs.

DEA&DP, 2019. Risk and Resilience Assessment of Natural Capital in the Greater Saldanha Bay Municipality: A Navigational Tool for Strategic-Level Decision-Making (No. 978- 0-621-47955–3). Western Cape Department of Environmental Affairs and Development Planning, Cape Town.

Dehghani, S., Moore, F., Keshavarzi, B., Hale, B., A., 2017. Health risk implications of potentially toxic metals in street dust and surface soil of Tehran, Iran. Ecotoxicology and Environmental Safety 136, 92–103. https://doi.org/10.1016/j.ecoenv.2016.10.037

Delgado-Iniesta, M.J., Marín-Sanleandro, P., Díaz-Pereira, E., Bautista, F., Romero-Muñoz, M., Sánchez-Navarro, A., 2022. Estimation of Ecological and Human Health Risks Posed by Heavy Metals in Street Dust of Madrid City (Spain). International Journal of Environmental Research and Public Health 19. https://doi.org/10.3390/ijerph19095263

Delibašić, Š., Đokić-Kahvedžić, N., Karić, M., Keskin, I., Velispahić, A., Huremović, J., Herceg, K., Selimović, A., Silajdžić, S., Žero, S., Gojak-Salimović, S., Partić, A., Pašalić, A., 2020. Health risk assessment of heavy metal contamination in street dust of federation of Bosnia and Herzegovina. Human and Ecological Risk Assessment: An International Journal 27, 1296–1308. https://doi.org/10.1080/10807039.2020.1826290

Drahota, P., Raus, K., Rychlíková, E., Rohovec, J., 2018. Bioaccessibility of As, Cu, Pb, and Zn in mine waste, urban soil, and road dust in the historical mining village of Kaňk, Czech Republic. Environmental Geochemistry and Health 40, 1495–1512. https://doi.org/10.1007/s10653-017-9999-1

Entwistle, J.A., Hursthouse, A.S., Reis, P.A.M., Stewart, A.G., 2019. Metalliferous Mine Dust: Human Health Impacts and the Potential Determinants of Disease in Mining Communities. Current Pollution Reports 5, 67–83. https://doi.org/10.1007/s40726-019-00108-5

González-Castanedo, Y., Sanchez-Rodas, D., De La Campa, A.S., Pandolfi, M., Alastuey, A., Cachorro, V., Querol, X., de La Rosa, J., 2015. Arsenic species in atmospheric particulate matter as tracer of the air quality of Doñana Natural Park (SW Spain). Chemosphere 119, 1296–1303.

Goossens, D., 2004. Effect of soil crusting on the emission and transport of wind-eroded sediment: field measurements on loamy sandy soil. Geomorphology 58, 145–160. https://doi.org/10.1016/S0169-555X(03)00229-0

Guney, M., Zagury, G.J., Dogan, N., Onay, T.T., 2010. Exposure assessment and risk characterization from trace elements following soil ingestion by children exposed to playgrounds, parks and picnic areas. Journal of Hazardous Materials 182, 656–664. https://doi.org/10.1016/j.jhazmat.2010.06.082

Han, F.X., Banin, A., Su, Y., Monts, D.L., Plodinec, J.M., Kingery, W.L., Triplett, G.E., 2002. Industrial age anthropogenic inputs of heavy metals into the pedosphere. Naturwissenschaften 89, 497–504. https://doi.org/10.1007/s00114-002-0373-4

Health Effects Institute, 2020. State of Global Air 2020. Special Report. Boston.

Hooper, J., Marx, S., 2018. A global doubling of dust emissions during the Anthropocene? Global and Planetary Change 169, 70–91. https://doi.org/10.1016/j.gloplacha.2018.07.003

Hu, X., Zhang, Y., Luo, J., Wang, T., Lian, H., Ding, Z., 2011. Bioaccessibility and health risk of arsenic, mercury and other metals in urban street dusts from a mega-city, Nanjing, China. Environmental Pollution 159, 1215–1221. https://doi.org/10.1016/j.envpol.2011.01.037

Huang, M., Chen, X., Zhao, Y., Chan, C.Y., Wang, W., Wang, X., Wong, M.H., 2014. Arsenic speciation in total contents and bioaccessible fractions in atmospheric particles related to human intakes. Environmental pollution 188, 37–44.

Jadoon, W.A., Abdel-Dayem, S.M.M.A., Saqib, Z., Takeda, K., Sakugawa, H., Hussain, M., Shah, G.M., Rehman, W., Syed, J.H., 2021. Heavy metals in urban dusts from Alexandria and Kafr El-Sheikh, Egypt: implications for human health. Environmental Science and Pollution Research 28, 2007–2018. https://doi.org/10.1007/s11356-020-08786-1

Kar, S., Maity, J.P., Samal, A.C., Santra, S.C., 2010. Metallic components of traffic-induced urban aerosol, their spatial variation, and source apportionment. Environmental Monitoring and Assessment 168, 561–574. https://doi.org/10.1007/s10661-009-1134-z

Keshavarzi, B., Tazarvi, Z., Rajabzadeh, M.A., Najmeddin, A., 2015. Chemical speciation, human health risk assessment and pollution level of selected heavy metals in urban street dust of Shiraz, Iran. Atmospheric Environment 119, 1–10. https://doi.org/10.1016/j.atmosenv.2015.08.001

Kurt-Karakus, P.B., 2012. Determination of heavy metals in indoor dust from Istanbul, Turkey: Estimation of the health risk. Environment International 50, 47–55. https://doi.org/10.1016/j.envint.2012.09.011

Landrigan, P.J., Gehlbach, S.H., Rosenblum, B.F., Shoults, J.M., Robert, P., Candelaria, M., Barthel, W.F., Liddle, J.A., Smrek, A.L., Staehling, N.W., others, 1975. Epidemic lead absorption near an ore smelter: the role of particulate lead. New England Journal of Medicine 292, 123–129.

Li, X.-D., Jin, L., Kan, H., 2019. Air pollution: a global problem needs local fixes. Nature 570, 437–439. https://doi.org/10.1038/d41586-019-01960-7

Li, Y., Ma, L., Ge, Y., Abuduwaili, J., 2022. Health risk of heavy metal exposure from dustfall and source apportionment with the PCA-MLR model: A case study in the Ebinur Lake Basin, China. Atmospheric Environment 272, 118950. https://doi.org/10.1016/j.atmosenv.2022.118950

Lin, Y., Zhang, X., Sun, Y., Cai, Z., Fu, F., 2022. Soluble arsenic species in total suspended particles and their health risk and origin implication: A case study in Taiyuan, China. Science of The Total Environment 807, 150791.

Ma, X., Xia, D., Liu, X., Liu, H., Fan, Y., Chen, P., Yu, Q., 2022. Application of magnetic susceptibility and heavy metal bioaccessibility to assessments of urban sandstorm contamination and health risks: Case studies from Dunhuang and Lanzhou, Northwest China. Science of The Total Environment 830, 154801. https://doi.org/10.1016/j.scitotenv.2022.154801

Mathee, A., 2014. Towards the prevention of lead exposure in South Africa: Contemporary and emerging challenges. NeuroToxicology 45, 220–223. https://doi.org/10.1016/j.neuro.2014.07.007

McConnell, J.R., Edwards, R., 2008. Coal burning leaves toxic heavy metal legacy in the Arctic. Proceedings of the National Academy of Sciences 105, 12140–12144. https://doi.org/10.1073/pnas.0803564105

Mendez, M.J., Funk, R., Buschiazzo, D.E., 2016. Efficiency of Big Spring Number Eight (BSNE) and Modified Wilson and Cook (MWAC) samplers to collect PM_{10}, $PM_{2.5}$ and PM_{1}. Aeolian Research 21, 37–44. https://doi.org/10.1016/j.aeolia.2016.02.003

Meza-Figueroa, D., Maier, R.M., de la O-Villanueva, M., Gómez-Alvarez, A., Moreno-Zazueta, A., Rivera, J., Campillo, A., Grandlic, C.J., Anaya, R., Palafox-Reyes, J., 2009. The impact of unconfined mine tailings in residential areas from a mining town in a semi-arid environment: Nacozari, Sonora, Mexico. Chemosphere 77, 140–147. https://doi.org/10.1016/j.chemosphere.2009.04.068

Mohmand, J., Eqani, S.A.M.A.S., Fasola, M., Alamdar, A., Mustafa, I., Ali, N., Liu, L., Peng, S., Shen, H., 2015. Human exposure to toxic metals via contaminated dust: Bio-accumulation trends and their potential risk estimation. Chemosphere 132, 142–151. https://doi.org/10.1016/j.chemosphere.2015.03.004

Mostafaii, G., Bakhtyari, Z., Atoof, F., Baziar, M., Fouladi-Fard, R., Rezaali, M., Mirzaei, N., 2021. Health risk assessment and source apportionment of heavy metals in atmospheric dustfall in a city of Khuzestan Province, Iran. Journal of Environmental Health Science and Engineering 19, 585–601. https://doi.org/10.1007/s40201-021-00630-z

Mvovo, I., Magagula, H.B., 2022. Health risks of heavy metal contamination in road surface dusts from selected major roads in East London, South Africa. International Journal of Environmental Health Research 32, 2425–2434. https://doi.org/10.1080/09603123.2021.1969340

Nan, N., Yan, Z., Zhang, Y., Chen, R., Qin, G., Sang, N., 2023. Overview of $PM_{2.5}$ and health outcomes: focusing on components, sources, and pollutant mixture co-exposure. Chemosphere 323, 138181.

Nelson, G., 2013. Occupational respiratory diseases in the South African mining industry. Global health action 6, 1–10. https://doi.org/10.3402/gha.v6i0.19520

NIOSH, H.D. of P.S., 1994. NIOSH, Manual of Analytical Methods. US Department of Health and Human Services, Public Health Service, Centers.

Nocoń, K., Rogula-Kozłowska, W., 2019. Speciation of arsenic: a case study of PM_1 in Zabrze. SN Applied Sciences 1, 450. https://doi.org/10.1007/s42452-019-0456-x

Nriagu, J.O., 1996. A History of Global Metal Pollution. Science 272, 223–223. https://doi.org/10.1126/science.272.5259.223

Okanigbe, D.O., Popoola, A.P.I., Adeleke, A.A., 2017. Characterization of Copper Smelter Dust for Copper Recovery. Procedia Manufacturing 7, 121–126. https://doi.org/10.1016/j.promfg.2016.12.032

Okorie, A., Entwistle, J., Dean, J.R., 2012. Estimation of daily intake of potentially toxic elements from urban street dust and the role of oral bioaccessibility testing. Chemosphere 86, 460–467. https://doi.org/10.1016/j.chemosphere.2011.09.047

Olowoyo, J.O., Lion, N., Unathi, T., Oladeji, O.M., 2022. Concentrations of Pb and Other Associated Elements in Soil Dust 15 Years after the Introduction of Unleaded Fuel and the Human Health Implications in Pretoria, South Africa. International Journal of Environmental Research and Public Health 19. https://doi.org/10.3390/ijerph191610238

Ondrasek, G., Shepherd, J., Rathod, S., Dharavath, R., Rashid, M.I., Brtnicky, M., Shahid, M.S., Horvatinec, J., Rengel, Z., 2025. Metal contamination–a global environmental issue: sources, implications & advances in mitigation. RSC advances 15, 3904–3927.

R Core Team, 2013. R: A Language and Environment for Statistical Computing. R Foundation for Statistical Computing, Vienna, Austria.

Rakhmatov, M., Abdullaev, S., 2021. The Content of Heavy Metals in Dust Aerosol and Soils of Northern Tajikistan. Atmospheric and Oceanic Optics 34, 212–221. https://doi.org/10.1134/S1024856021030118

Rani, N., Sastry, B.S., Dey, K., 2019. Assessment of metal contamination and the associated human health risk from dustfall deposition: a study in a mid-sized town in India. Environmental Science and Pollution Research 26, 23173–23191. https://doi.org/10.1007/s11356-019-05539-7

Safiur Rahman, M., Khan, M.D.H., Jolly, Y.N., Kabir, J., Akter, S., Salam, A., 2019. Assessing risk to human health for heavy metal contamination through street dust in the Southeast Asian Megacity: Dhaka, Bangladesh. Science of The Total Environment 660, 1610–1622. https://doi.org/10.1016/j.scitotenv.2018.12.425

Sánchez-Rodas, D., Sánchez de la Campa, A.M., de la Rosa, J.D., Oliveira, V., Gómez-Ariza, J.L., Querol, X., Alastuey, A., 2007. Arsenic speciation of atmospheric particulate matter (PM_{10}) in an industrialised urban site in southwestern Spain. Chemosphere 66, 1485–1493. https://doi.org/10.1016/j.chemosphere.2006.08.043

Soleimani-Sardo, M., Shirani, M., Strezov, V., 2023. Heavy metal pollution levels and health risk assessment of dust storms in Jazmurian region, Iran. Scientific Reports 13, 7337. https://doi.org/10.1038/s41598-023-34318-1

Soto-Jiménez, M.F., Flegal, A.R., 2011. Childhood lead poisoning from the smelter in Torreón, México. Environmental Research 111, 590–596. https://doi.org/10.1016/j.envres.2011.01.020

Stanin, F.T., 2005. The transport and fate of chromium (VI) in the environment. CRC Press, Florida, USA.

Świetlik, R., Molik, A., Molenda, M., Trojanowska, M., Siwiec, J., 2011. Chromium (III/VI) speciation in urban aerosol. Atmospheric Environment - ATMOS ENVIRON 45, 1364–1368. https://doi.org/10.1016/j.atmosenv.2010.12.001

Tanda, S., Gingl, K., Licbinsky, R., Hegrova, J., Goessler, W., 2020. Occurrence, Seasonal Variation and Size Resolved Distribution of Arsenic Species in Atmospheric Particulate Matter in an Urban Area in Southeastern Austria. Environmental Science & Technology XXXX. https://doi.org/10.1021/acs.est.9b07707

Tapia, J., Valdes, J., Orrego, R., Tchernitchin, A., Dorador, C., Bolados, A., Harrod, C., 2018. Geologic and anthropogenic sources of contamination in settled dust of a historic mining port city in northern Chile: Health risk implications. PeerJ 6, e4699. https://doi.org/10.7717/peerj.4699

Tian, H.Z., Zhu, C.Y., Gao, J.J., Cheng, K., Hao, J.M., Wang, K., Hua, S.B., Wang, Y., Zhou, J.R., 2015. Quantitative assessment of atmospheric emissions of toxic heavy metals from anthropogenic sources in China: historical trend, spatial distribution, uncertainties, and control policies. Atmospheric Chemistry and Physics 15, 10127–10147. https://doi.org/10.5194/acp-15-10127-2015

Tirez, K., Vanhoof, C., Peters, J., Geerts, L., Bleux, N., Adriaenssens, E., Roekens, E., Smolek, S., Maderitsch, A., Steininger, R., others, 2015. Speciation of inorganic arsenic in particulate matter by combining HPLC/ICP-MS and XANES analyses. Journal of Analytical Atomic Spectrometry 30, 2074–2088.

Torkmahalleh, M.A., Yu, C.-H., Lin, L., Fan, Z. (Tina), Swift, J.L., Bonanno, L., Rasmussen, D.H., Holsen, T.M., Hopke, P.K., 2013. Improved atmospheric sampling of hexavalent chromium. Journal of the Air & Waste Management Association 63, 1313–1323. https://doi.org/10.1080/10962247.2013.823894

Trojanowska, M., Świetlik, R., 2020. Investigations of the chemical distribution of heavy metals in street dust and its

impact on risk assessment for human health, case study of Radom (Poland). Human and Ecological Risk Assessment: An International Journal 26, 1907–1926. https://doi.org/10.1080/10807039.2019.1619070

US EPA, 2023. United States Environmental Protection Agency. Regional Screening Levels for Chemical Contaminants at Superfund Sites.

US EPA, 2011. Exposure factors handbook. Office of research and Development, Washington, DC 20460, 2–6.

US EPA, 2001. Supplemental Guidance for Developing Soil Screening Levels for Superfund Sites (No. OSWER 9355.4-24). Office of Soild Waste and Emergency Response.

US EPA, 1996. Soil screening guidance: Technical background document. EPA/540/R-95/128.

US EPA, 1989. Risk Assessment Guidance for Superfund: pt. A. Human health evaluation manual. Office of Emergency and Remedial Response, US Environmental Protection Agency.

Utembe, W., Faustman, E., Matatiele, P., Mary, G., 2015. Hazards identified and the need for health risk assessment in the South African mining industry. Human & Experimental Toxicology 34, 1212–1221. https://doi.org/10.1177/0960327115600370

van den Berg, R., 1994. Human exposure to soil contamination: a qualitative and quantitative analysis towards proposals for human toxicological intervention values (partly revised edition).

Vos, H.C., Kangueehi, K.I., Toesie, R., Eckardt, F.D., Ravenscroft, G., Fietz, S., 2024. Spatial variability of dust concentration and deposition around an industrial port in South Africa emphasises the complexity of sources and transport. Air Quality, Atmosphere & Health. https://doi.org/10.1007/s11869-024-01581-8

Wan, D., Song, L., Yang, J., Jin, Z., Zhan, C., Mao, X., Liu, D., Shao, Y., 2016. Increasing heavy metals in the background atmosphere of central North China since the 1980s: Evidence from a 200-year lake sediment record. Atmospheric Environment 138, 183–190. https://doi.org/10.1016/j.atmosenv.2016.05.015

Wang, J., Huang, Y., Li, T., He, M., Cheng, X., Su, T., Ni, S., Zhang, C., 2020. Contamination, morphological status and sources of atmospheric dust in different land-using areas of a steel-industry city, China. Atmospheric Pollution Research 11, 283–289. https://doi.org/10.1016/j.apr.2019.10.014

Wei, T., Simko, V., 2021. R package "corrplot": Visualization of a Correlation Matrix.

WHO, 2021. WHO global air quality guidelines: particulate matter ($PM_{2.5}$ and PM_{10}), ozone, nitrogen dioxide, sulfur dioxide and carbon monoxide. World Health Organization.

WHO, 2017. Guidelines for drinking-water quality: fourth edition incorporating the first addendum.

WHO, 2016. Ambient air pollution: a global assessment of exposure and burden of disease. World Health Organization, Geneva.

Wickham, H., 2016. ggplot2: Elegant Graphics for Data Analysis. Springer-Verlag New York.

Yan, J., Li, Z., Wang, K., Xie, C., Zhu, J., Wu, S., 2025. Association between ambient fine particulate matter constituents and mortality and morbidity of cardiovascular and respiratory diseases: A systematic review and meta-analysis. Environmental Pollution 126476.

Yang, X., Wang, M., He, Q., Mamtimin, A., Huo, W., Yang, F., Zhou, C., 2018. Estimation of sampling efficiency of the Big Spring Number Eight (BSNE) sampler at different heights based on sand particle size in the Taklimakan Desert. Geomorphology 322, 89–96. https://doi.org/10.1016/j.geomorph.2018.08.042

Yu, C.H., Huang, L., Shin, J.Y., Artigas, F., Fan, Z., 2014. Characterization of Concentration, Particle Size Distribution, and Contributing Factors to Ambient Hexavalent Chromium in an Area with Multiple Emission Sources. Atmospheric Environment 94. https://doi.org/10.1016/j.atmosenv.2014.06.004

Zhaoyong, Z., Mamat, A., Simayi, Z., 2019. Pollution assessment and health risks evaluation of (metalloid) heavy metals in urban street dust of 58 cities in China. Environmental Science and Pollution Research 26, 126–140. https://doi.org/10.1007/s11356-018-3555-0

Zheng, N., Hou, S., Wang, S., Sun, S., An, Q., Li, P., Li, X., 2020. Health risk assessment of heavy metals in street dust around a zinc smelting plant in China based on bioavailability and bioaccessibility. Ecotoxicology and Environmental Safety 197, 110617. https://doi.org/10.1016/j.ecoenv.2020.110617

Zheng, N., Liu, J., Wang, Q., Liang, Z., 2010. Health risk assessment of heavy metal exposure to street dust in the zinc smelting district, Northeast of China. Science of The Total Environment 408, 726–733. https://doi.org/10.1016/j.scitotenv.2009.10.075

Supplementary material

Supplementary material can be accessed at https://cleanairjournal.org.za/article/view/22227